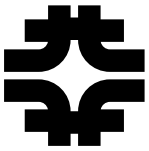

Fermi National Accelerator Laboratory

FERMILAB-Pub-98/167-E
CDF

Improved Measurement of the B^- and $\bar{B}^0$ Meson Lifetimes Using Semileptonic Decays

F. Abe et al.
The CDF Collaboration

Fermi National Accelerator Laboratory
P.O. Box 500, Batavia, Illinois 60510

June 1998

Submitted to *Physical Review D*

Operated by Universities Research Association Inc. under Contract No. DE-AC02-76CH03000 with the United States Department of Energy

Disclaimer

Distribution

CDF/PUB/BOTTOM/PUBLIC/4534
FERMILAB-Pub-98/167-E
June 14, 1998

Improved measurement of the B^- and $\overline{B}^0$ meson lifetimes using semileptonic decays *

F. Abe,[17] H. Akimoto,[39] A. Akopian,[31] M. G. Albrow,[7] A. Amadon,[5] S. R. Amendolia,[27] D. Amidei,[20] J. Antos,[33] S. Aota,[37] G. Apollinari,[31] T. Arisawa,[39] T. Asakawa,[37] W. Ashmanskas,[18] M. Atac,[7] P. Azzi-Bacchetta,[25] N. Bacchetta,[25] S. Bagdasarov,[31] M. W. Bailey,[22] P. de Barbaro,[30] A. Barbaro-Galtieri,[18] V. E. Barnes,[29] B. A. Barnett,[15] M. Barone,[9] G. Bauer,[19] T. Baumann,[11] F. Bedeschi,[27] S. Behrends,[3] S. Belforte,[27] G. Bellettini,[27] J. Bellinger,[40] D. Benjamin,[35] J. Bensinger,[3] A. Beretvas,[7] J. P. Berge,[7] J. Berryhill,[5] S. Bertolucci,[9] S. Bettelli,[27] B. Bevensee,[26] A. Bhatti,[31] K. Biery,[7] C. Bigongiari,[27] M. Binkley,[7] D. Bisello,[25] R. E. Blair,[1] C. Blocker,[3] S. Blusk,[30] A. Bodek,[30] W. Bokhari,[26] G. Bolla,[29] Y. Bonushkin,[4] D. Bortoletto,[29] J. Boudreau,[28] L. Breccia,[2] C. Bromberg,[21] N. Bruner,[22] R. Brunetti,[2] E. Buckley-Geer,[7] H. S. Budd,[30] K. Burkett,[20] G. Busetto,[25] A. Byon-Wagner,[7] K. L. Byrum,[1] M. Campbell,[20] A. Caner,[27] W. Carithers,[18] D. Carlsmith,[40] J. Cassada,[30] A. Castro,[25] D. Cauz,[36] A. Cerri,[27] P. S. Chang,[33] P. T. Chang,[33] H. Y. Chao,[33] J. Chapman,[20] M. -T. Cheng,[33] M. Chertok,[34] G. Chiarelli,[27] C. N. Chiou,[33] F. Chlebana,[7] L. Christofek,[13] M. L. Chu,[33] S. Cihangir,[7] A. G. Clark,[10] M. Cobal,[27] E. Cocca,[27] M. Contreras,[5] J. Conway,[32] J. Cooper,[7] M. Cordelli,[9] D. Costanzo,[27] C. Couyoumtzelis,[10] D. Cronin-Hennessy,[6] R. Culbertson,[5] D. Dagenhart,[38] T. Daniels,[19] F. DeJongh,[7] S. Dell'Agnello,[9] M. Dell'Orso,[27] R. Demina,[7] L. Demortier,[31] M. Deninno,[2] P. F. Derwent,[7] T. Devlin,[32] J. R. Dittmann,[6] S. Donati,[27] J. Done,[34] T. Dorigo,[25] N. Eddy,[20] K. Einsweiler,[18] J. E. Elias,[7] R. Ely,[18] E. Engels, Jr.,[28] W. Erdmann,[7]

*Submitted to *Physical Review D.*

D. Errede,[13] S. Errede,[13] Q. Fan,[30] R. G. Feild,[41] Z. Feng,[15] C. Ferretti,[27] I. Fiori,[2] B. Flaugher,[7] G. W. Foster,[7] M. Franklin,[11] J. Freeman,[7] J. Friedman,[19] H. Frisch,[5] Y. Fukui,[17] S. Gadomski,[14] S. Galeotti,[27] M. Gallinaro,[26] O. Ganel,[35] M. Garcia-Sciveres,[18] A. F. Garfinkel,[29] C. Gay,[41] S. Geer,[7] D. W. Gerdes,[15] P. Giannetti,[27] N. Giokaris,[31] P. Giromini,[9] G. Giusti,[27] M. Gold,[22] A. Gordon,[11] A. T. Goshaw,[6] Y. Gotra,[28] K. Goulianos,[31] H. Grassmann,[36] L. Groer,[32] C. Grosso-Pilcher,[5] G. Guillian,[20] J. Guimaraes da Costa,[15] R. S. Guo,[33] C. Haber,[18] E. Hafen,[19] S. R. Hahn,[7] R. Hamilton,[11] T. Handa,[12] R. Handler,[40] F. Happacher,[9] K. Hara,[37] A. D. Hardman,[29] R. M. Harris,[7] F. Hartmann,[16] J. Hauser,[4] E. Hayashi,[37] J. Heinrich,[26] W. Hao,[35] B. Hinrichsen,[14] K. D. Hoffman,[29] M. Hohlmann,[5] C. Holck,[26] R. Hollebeek,[26] L. Holloway,[13] Z. Huang,[20] B. T. Huffman,[28] R. Hughes,[23] J. Huston,[21] J. Huth,[11] H. Ikeda,[37] M. Incagli,[27] J. Incandela,[7] G. Introzzi,[27] J. Iwai,[39] Y. Iwata,[12] E. James,[20] H. Jensen,[7] U. Joshi,[7] E. Kajfasz,[25] H. Kambara,[10] T. Kamon,[34] T. Kaneko,[37] K. Karr,[38] H. Kasha,[41] Y. Kato,[24] T. A. Keaffaber,[29] K. Kelley,[19] R. D. Kennedy,[7] R. Kephart,[7] D. Kestenbaum,[11] D. Khazins,[6] T. Kikuchi,[37] B. J. Kim,[27] H. S. Kim,[14] S. H. Kim,[37] Y. K. Kim,[18] L. Kirsch,[3] S. Klimenko,[8] D. Knoblauch,[16] P. Koehn,[23] A. Köngeter,[16] K. Kondo,[37] J. Konigsberg,[8] K. Kordas,[14] A. Korytov,[8] E. Kovacs,[1] W. Kowald,[6] J. Kroll,[26] M. Kruse,[30] S. E. Kuhlmann,[1] E. Kuns,[32] K. Kurino,[12] T. Kuwabara,[37] A. T. Laasanen,[29] S. Lami,[27] S. Lammel,[7] J. I. Lamoureux,[3] M. Lancaster,[18] M. Lanzoni,[27] G. Latino,[27] T. LeCompte,[1] S. Leone,[27] J. D. Lewis,[7] P. Limon,[7] M. Lindgren,[4] T. M. Liss,[13] J. B. Liu,[30] Y. C. Liu,[33] N. Lockyer,[26] O. Long,[26] C. Loomis,[32] M. Loreti,[25] D. Lucchesi,[27] P. Lukens,[7] S. Lusin,[40] J. Lys,[18] K. Maeshima,[7] P. Maksimovic,[11] M. Mangano,[27] M. Mariotti,[25] J. P. Marriner,[7] G. Martignon,[25] A. Martin,[41] J. A. J. Matthews,[22] P. Mazzanti,[2] P. McIntyre,[34] P. Melese,[31] M. Menguzzato,[25] A. Menzione,[27] E. Meschi,[27] S. Metzler,[26] C. Miao,[20] T. Miao,[7] G. Michail,[11] R. Miller,[21] H. Minato,[37] S. Miscetti,[9] M. Mishina,[17] S. Miyashita,[37] N. Moggi,[27] E. Moore,[22] Y. Morita,[17] A. Mukherjee,[7] T. Muller,[16] P. Murat,[27] S. Murgia,[21] M. Musy,[36] H. Nakada,[37] I. Nakano,[12] C. Nelson,[7] D. Neuberger,[16] C. Newman-Holmes,[7] C.-Y. P. Ngan,[19] L. Nodulman,[1] A. Nomerotski,[8] S. H. Oh,[6] T. Ohmoto,[12] T. Ohsugi,[12] R. Oishi,[37] M. Okabe,[37] T. Okusawa,[24] J. Olsen,[40] C. Pagliarone,[27] R. Paoletti,[27] V. Papadimitriou,[35] S. P. Pappas,[41] N. Parashar,[27]

A. Parri,[9] J. Patrick,[7] G. Pauletta,[36] M. Paulini,[18] A. Perazzo,[27] L. Pescara,[25] M. D. Peters,[18] T. J. Phillips,[6] G. Piacentino,[27] M. Pillai,[30] K. T. Pitts,[7] R. Plunkett,[7] A. Pompos,[29] L. Pondrom,[40] J. Proudfoot,[1] F. Ptohos,[11] G. Punzi,[27] K. Ragan,[14] D. Reher,[18] M. Reischl,[16] A. Ribon,[25] F. Rimondi,[2] L. Ristori,[27] W. J. Robertson,[6] T. Rodrigo,[27] S. Rolli,[38] L. Rosenson,[19] R. Roser,[13] T. Saab,[14] W. K. Sakumoto,[30] D. Saltzberg,[4] A. Sansoni,[9] L. Santi,[36] H. Sato,[37] P. Schlabach,[7] E. E. Schmidt,[7] M. P. Schmidt,[41] A. Scott,[4] A. Scribano,[27] S. Segler,[7] S. Seidel,[22] Y. Seiya,[37] F. Semeria,[2] T. Shah,[19] M. D. Shapiro,[18] N. M. Shaw,[29] P. F. Shepard,[28] T. Shibayama,[37] M. Shimojima,[37] M. Shochet,[5] J. Siegrist,[18] A. Sill,[35] P. Sinervo,[14] P. Singh,[13] K. Sliwa,[38] C. Smith,[15] F. D. Snider,[15] J. Spalding,[7] T. Speer,[10] P. Sphicas,[19] F. Spinella,[27] M. Spiropulu,[11] L. Spiegel,[7] L. Stanco,[25] J. Steele,[40] A. Stefanini,[27] R. Ströhmer,[7a] J. Strologas,[13] F. Strumia, [10] D. Stuart,[7] K. Sumorok,[19] J. Suzuki,[37] T. Suzuki,[37] T. Takahashi,[24] T. Takano,[24] R. Takashima,[12] K. Takikawa,[37] M. Tanaka,[37] B. Tannenbaum,[22] F. Tartarelli,[27] W. Taylor,[14] M. Tecchio,[20] P. K. Teng,[33] Y. Teramoto,[24] K. Terashi,[37] S. Tether,[19] D. Theriot,[7] T. L. Thomas,[22] R. Thurman-Keup,[1] M. Timko,[38] P. Tipton,[30] A. Titov,[31] S. Tkaczyk,[7] D. Toback,[5] K. Tollefson,[19] A. Tollestrup,[7] H. Toyoda,[24] W. Trischuk,[14] J. F. de Troconiz,[11] S. Truitt,[20] J. Tseng,[19] N. Turini,[27] T. Uchida,[37] F. Ukegawa,[26] J. Valls,[32] S. C. van den Brink,[28] S. Vejcik, III,[20] G. Velev,[27] R. Vidal,[7] R. Vilar,[7a] D. Vucinic,[19] R. G. Wagner,[1] R. L. Wagner,[7] J. Wahl,[5] N. B. Wallace,[27] A. M. Walsh,[32] C. Wang,[6] C. H. Wang,[33] M. J. Wang,[33] A. Warburton,[14] T. Watanabe,[37] T. Watts,[32] R. Webb,[34] C. Wei,[6] H. Wenzel,[16] W. C. Wester, III,[7] A. B. Wicklund,[1] E. Wicklund,[7] R. Wilkinson,[26] H. H. Williams,[26] P. Wilson,[5] B. L. Winer,[23] D. Winn,[20] D. Wolinski,[20] J. Wolinski,[21] S. Worm,[22] X. Wu,[10] J. Wyss,[27] A. Yagil,[7] W. Yao,[18] K. Yasuoka,[37] G. P. Yeh,[7] P. Yeh,[33] J. Yoh,[7] C. Yosef,[21] T. Yoshida,[24] I. Yu,[7] A. Zanetti,[36] F. Zetti,[27] and S. Zucchelli[2]

(CDF Collaboration)

[1] *Argonne National Laboratory, Argonne, Illinois 60439*

[2] *Istituto Nazionale di Fisica Nucleare, University of Bologna, I-40127 Bologna, Italy*

[3] *Brandeis University, Waltham, Massachusetts 02254*

[4] *University of California at Los Angeles, Los Angeles, California 90024*

[5] *University of Chicago, Chicago, Illinois 60637*

[6] *Duke University, Durham, North Carolina 27708*

[7] *Fermi National Accelerator Laboratory, Batavia, Illinois 60510*

[8] *University of Florida, Gainesville, FL 32611*

[9] *Laboratori Nazionali di Frascati, Istituto Nazionale di Fisica Nucleare, I-00044 Frascati, Italy*

[10] *University of Geneva, CH-1211 Geneva 4, Switzerland*

[11] *Harvard University, Cambridge, Massachusetts 02138*

[12] *Hiroshima University, Higashi-Hiroshima 724, Japan*

[13] *University of Illinois, Urbana, Illinois 61801*

[14] *Institute of Particle Physics, McGill University, Montreal H3A 2T8, and University of Toronto, Toronto M5S 1A7, Canada*

[15] *The Johns Hopkins University, Baltimore, Maryland 21218*

[16] *Institut für Experimentelle Kernphysik, Universität Karlsruhe, 76128 Karlsruhe, Germany*

[17] *National Laboratory for High Energy Physics (KEK), Tsukuba, Ibaraki 305, Japan*

[18] *Ernest Orlando Lawrence Berkeley National Laboratory, Berkeley, California 94720*

[19] *Massachusetts Institute of Technology, Cambridge, Massachusetts 02139*

[20] *University of Michigan, Ann Arbor, Michigan 48109*

[21] *Michigan State University, East Lansing, Michigan 48824*

[22] *University of New Mexico, Albuquerque, New Mexico 87131*

[23] *The Ohio State University, Columbus, OH 43210*

[24] *Osaka City University, Osaka 588, Japan*

[25] *Universita di Padova, Istituto Nazionale di Fisica Nucleare, Sezione di Padova, I-35131 Padova, Italy*

[26] *University of Pennsylvania, Philadelphia, Pennsylvania 19104*

[27] *Istituto Nazionale di Fisica Nucleare, University and Scuola Normale Superiore of Pisa, I-56100 Pisa, Italy*

[28] *University of Pittsburgh, Pittsburgh, Pennsylvania 15260*

[29] *Purdue University, West Lafayette, Indiana 47907*

[30] *University of Rochester, Rochester, New York 14627*

[31] *Rockefeller University, New York, New York 10021*

[32] *Rutgers University, Piscataway, New Jersey 08855*

[33] *Academia Sinica, Taipei, Taiwan 11530, Republic of China*

[34] *Texas A&M University, College Station, Texas 77843*

[35] *Texas Tech University, Lubbock, Texas 79409*

[36] *Istituto Nazionale di Fisica Nucleare, University of Trieste/ Udine, Italy*

[37] *University of Tsukuba, Tsukuba, Ibaraki 315, Japan*

[38] *Tufts University, Medford, Massachusetts 02155*

[39] *Waseda University, Tokyo 169, Japan*

[40] *University of Wisconsin, Madison, Wisconsin 53706*

[41] *Yale University, New Haven, Connecticut 06520*

Abstract

The lifetimes of the B^- and $\overline{B}^0$ mesons are measured using the partially reconstructed semileptonic decays $\overline{B} \to D\ell^-\overline{\nu}X$, where D is either a D^0 or D^{*+} meson. The data were collected by the CDF detector at the Fermilab Tevatron collider during 1992-1995 and correspond to about 110 pb^{-1} of $\bar{p}p$ collisions at $\sqrt{s} = 1.8$ TeV. We measure decay lengths and extract the lifetimes to be $\tau(B^-) = 1.637 \pm 0.058 \,^{+0.045}_{-0.043}$ ps and $\tau(\overline{B}^0) = 1.474 \pm 0.039 \,^{+0.052}_{-0.051}$ ps, and the ratio of the lifetimes to be $\tau(B^-)/\tau(\overline{B}^0) = 1.110 \pm 0.056 \,^{+0.033}_{-0.030}$, where the first uncertainties are statistical and the second are systematic.

PACS numbers: 13.20.He, 14.40.Nd

I. INTRODUCTION

Measurements of the lifetimes of the individual B-hadron species can probe their decay mechanism beyond the simple spectator model decay picture. In this model, all hadrons containing a heavy quark should have one identical lifetime, that of the quark. However, this picture does not hold in the case of charm hadrons; the lifetimes of D^+ and D^0 mesons differ by a factor of 2.5. Possible causes of lifetime differences include contributions from non-spectator decays, namely the annihilation and the W-exchange processes, and so-called final-state Pauli interference effects. Obviously, these mechanisms play an important role in the decay of charm hadrons. However, they are expected to produce smaller lifetime differences between the B hadrons because of the larger mass of the b quark.

In the past few years, the heavy quark expansion technique has been applied extensively to the calculations of inclusive decay rates of heavy hadrons, both spectator and non-spectator decays. It provides quantitative predictions for lifetime differences among the heavy hadrons. It is generally believed that there should exist a lifetime difference of order (5-10)% between

the B^- and $\overline{B}^0$ mesons. Bigi predicts [1] that the B^- meson lifetime should be longer than the $\overline{B}^0$ meson lifetime. However, Neubert and Sachrajda [2] state that the sign of the deviation from unity cannot be predicted reliably. A much smaller difference, of order 1%, is predicted for the $\overline{B}^0$ and $\overline{B}_s^0$ meson lifetimes.

Several direct measurements of B^- and $\overline{B}^0$ meson lifetimes have been performed recently by the e^+e^- experiments [3] and by CDF [4,5]. Indirect information has been obtained through the measurement of branching fractions [6]. The precision of current measurements now approaches the level where the predicted small differences could be discerned, and improvements in these measurements will provide a strong test of B-hadron decay mechanisms.

In this Article we report a measurement of the B^- and $\overline{B}^0$ meson lifetimes using partially reconstructed semileptonic decays. The data used in this analysis were collected in 1992-95 with the CDF detector at the Fermilab Tevatron proton-antiproton collider at a center-of-mass energy $\sqrt{s} = 1.8$ TeV and correspond to an integrated luminosity of about 110 pb^{-1}.

In order to identify semileptonic decays of B mesons, events with a lepton (e^- or μ^-, denoted by ℓ^-) associated with a D^0 or D^{*+} meson are selected. (Throughout this Article a reference to a particular charge state also implies its charge conjugate.) The $\ell^- D^0$ candidates consist mostly of B^- decays, and the $\ell^- D^{*+}$ candidates consist mostly of $\overline{B}^0$ decays. The D^0 mesons are reconstructed using the decay mode $D^0 \to K^-\pi^+$. The D^{*+} decays are reconstructed using the decay mode $D^{*+} \to D^0\pi^+$, followed by $D^0 \to K^-\pi^+$, $K^-\pi^+\pi^+\pi^-$ or $K^-\pi^+\pi^0$. About 6000 such decays are reconstructed in the data sample. The decay length distributions are measured and the lifetimes are extracted after correcting for the relative admixtures of B^- and $\overline{B}^0$ mesons in the samples. The results presented here supersede a previous CDF measurement [4], since the part of the data sample used here is the same as that of Ref. [4].

II. CDF DETECTOR AND TRIGGER

The CDF detector is described in detail elsewhere [7]. We describe here only the detector components most relevant to this analysis. Inside the 1.4 T solenoid the silicon vertex de-

tector (SVX) and the central tracking chamber (CTC) provide the tracking and momentum analysis of charged particles. The CTC is a cylindrical drift chamber containing 84 measurement layers. It covers the pseudorapidity interval $|\eta| < 1.1$, where $\eta = -\ln[\tan(\theta/2)]$ [8]. The SVX consists of four layers of silicon micro-strip detectors located at radii between 3.0 and 7.9 cm from the interaction point and provides spatial measurements in the r-φ plane with a resolution of 13 μm. It gives a track impact parameter resolution of about $(13+40/p_T)$ μm [9], where $p_{\rm T}$ is the transverse momentum of the track measured in GeV/c. The geometric acceptance of the SVX is $\sim 60\%$, as it extends to $\pm$ 25 cm from the nominal interaction point, whereas the position of the primary interaction vertices has an rms width of ~ 30 cm along the beam (z) direction. The transverse profile of the Tevatron beam is circular and has an rms spread of ~ 35 μm for the data taking period in 1992-93 and ~ 25 μm in 1994-95. The p_T resolution of the CTC combined with the SVX is $\sigma(p_T)/p_T = [(0.0066)^2 + (0.0009\,p_T)^2]^{1/2}$. Electromagnetic (CEM) and hadronic (CHA) calorimeters with projective tower geometry are located outside the solenoid and cover the pseudorapidity region $|\eta| < 1.1$, with a segmentation of $\Delta\varphi = 15^\circ$ and $\Delta\eta \simeq 0.11$. A layer of proportional chambers (CES) is embedded near shower maximum in the CEM and provides a more precise measurement of electromagnetic shower profiles and an additional measurement of pulse height. Also, a layer of proportional chambers (CPR) is installed between the solenoid and the CEM, and samples electromagnetic showers at about one radiation length. Two muon subsystems in the central rapidity region are used for muon identification. The central muon chambers (CMU) are located just behind the CHA calorimeter, and the central upgrade muon chambers (CMP) follow an additional 60 cm of steel.

Events containing semileptonic B decays are collected using inclusive lepton triggers. CDF uses a three-level trigger system, where at the first two levels decisions are made with dedicated hardware. The information available at this stage includes energy deposits in the CEM and CHA calorimeters, high p_T tracks found in CTC by a track processor, and track segments found in the muon subsystems. The E_T threshold for the principal single electron trigger is 9 (8) GeV for the data taking period in 1992-93 (94-95), where $E_T \equiv E \sin\theta$, and E is the energy measured in the CEM. In addition, a track is required in the CTC with $p_T > 7.5$

GeV/c that points at the calorimeter tower in φ. For the 1994-95 data taking period the CES was added to the trigger system [10]. The electron trigger requires the presence of pulse height in the CES corresponding to an electromagnetic shower of 4 GeV or above. Also, the φ position of the shower is available with a segmentation of $\Delta\varphi = 2°$, and the CTC track is required to point at the shower. The single muon trigger requires a track in the CTC, corresponding to a particle with $p_T > 7.5$ GeV/c, and track segments in both the CMU and CMP systems that match the CTC track within 7.5° in φ. At the third level of the trigger, the event selection is based on a version of off-line reconstruction programs optimized for speed. The lepton selection criteria used in level 3 are similar to those described in the next Section.

III. RECONSTRUCTION OF SEMILEPTONIC DECAYS OF B MESONS

The analysis starts with identification of leptons, e^- or μ^-. If an event contains a good lepton candidate, we look for the charm meson D^0 or D^{*+} produced in the vicinity of the lepton candidate, to be consistent with the semileptonic decay signature $\overline{B} \to \ell^- \bar{\nu} D X$. A proper correlation between the lepton charge and the charm flavor, ℓ^- with D, not ℓ^+ with D, is required.

A. Lepton Identification

The identification of electrons makes use of information from both calorimeters and tracking chambers. To be specific we require the following:

- Longitudinal profile consistent with an electron shower, i.e. small leakage energy in the CHA.
- Lateral shower profiles measured in the CEM [11] and the CES [12] consistent with electron test beam data.

- Association of a high p_T track with the calorimeter shower based on position matching and energy-to-momentum ratio.

- Pulse heights in the CES and CPR consistent with an electron.

Photon conversion electrons, as well as Dalitz decays of π^0 mesons, are removed by looking for oppositely charged tracks that have small opening angles with the electron candidate.

Muons are identified based on the geometrical matching between the track segments in the muon chambers and an extrapolated CTC track. We compute the χ^2 of the matching, where the uncertainty is dominated by multiple Coulomb scattering in the detector material. We require $\chi^2 < 9$ in the r-φ view (CMU and CMP) and $\chi^2 < 12$ in the r-z view (CMU).

B. Charm meson reconstruction

To identify the $\ell^- D^0$ candidates, we search for $D^0 \to K^-\pi^+$ decays near the leptons, removing events that are consistent with the $D^{*+} \to D^0\pi^+$ decay chain. The $D^0 \to K^-\pi^+$ decay is reconstructed as follows. We first select oppositely charged pairs of particles using CTC tracks, where the kaon mass is assigned to the particle with the same charge as the lepton (called the "right sign" combination), as is the case in semileptonic B decays. The kaon (pion) candidate is then required to have momentum above 1.5 (0.5) GeV/c, and to be within a cone of radius $\Delta R = 0.6$ (0.7) around the lepton in η-φ space, where $\Delta R = \sqrt{(\Delta\eta)^2 + (\Delta\varphi)^2}$. To ensure accurate decay length measurement, each candidate track is required to be reconstructed in the SVX, as well as the lepton track. To reduce combinatorial background, we require the decay vertex of the D^0 candidate to be positively displaced along its flight direction in the transverse plane with respect to the position of the primary vertex. The primary vertex is approximated by the beam position [5,13]. To remove events consistent with the decay chain $D^{*+} \to D^0\pi^+$, we combine additional positive tracks with the D^0 candidate and compute the mass difference (Δm) between the $D^0\pi^+$ and the D^0, assigning the pion mass to the tracks. The Δm resolution is measured to be 0.74 MeV/c^2. We remove the D^0 candidate if any track exists that gives a Δm value between 0.142 and 0.148 GeV/c^2. The resulting $K^-\pi^+$ invariant mass spectrum is shown in Fig. 1(a). We

fit a polynomial background and a Gaussian distribution to the spectrum and find a mass resolution of 11.3 MeV/c^2. Also shown by the shaded histogram is the mass spectrum for the "wrong sign" ($K^+\pi^-$ with ℓ^-) combinations, where no significant signal is observed. We define the signal region to be in the mass range from 1.84 to 1.88 GeV/c^2. The total number of events in the signal region is 5198, and the background fraction is estimated from the fit to be 0.53 ± 0.02.

To identify $\ell^- D^{*+}$ candidates, we search for $D^{*+} \to D^0\pi^+$ decays using two fully reconstructed D^0 decay modes, $D^0 \to K^-\pi^+$ and $D^0 \to K^-\pi^+\pi^+\pi^-$, and one partially reconstructed mode, $D^0 \to K^-\pi^+\pi^0$. For the $D^0 \to K^-\pi^+$ and $K^-\pi^+\pi^0$ modes, we apply the same momentum and cone requirements to the kaon and pion candidates as in the $\overline{B} \to \ell^- D^0 X$ reconstruction. For the $D^0 \to K^-\pi^+\pi^+\pi^-$ mode, the kaon (pion) candidate is required to have momentum above 1.2 (0.5) GeV/c, and to be within a cone of radius 0.65 (1.0) around the lepton candidate. Also, we require the decay vertex of the D^0 candidate to be positively displaced with respect to the primary vertex in the $D^0 \to K^-\pi^+\pi^+\pi^-$ and $K^-\pi^+\pi^0$ modes. For the fully reconstructed modes, the D^0 candidate has to be in the mass ranges 1.83 to 1.90 GeV/c^2 and 1.84 to 1.88 GeV/c^2, respectively. For the partially reconstructed mode, we require the mass of a $K^-\pi^+$ pair to be between 1.5 and 1.7 GeV/c^2; we do not reconstruct the π^0 and in the subsequent analysis treat the $K^-\pi^+$ pair as if it were a D^0. For each mode, we reconstruct the D^{*+} meson by combining an additional track, assumed to have the pion mass, with the D^0 candidate, and computing the mass difference, Δm, between the $D^0\pi^+$ and D^0 candidates. Figures 1(b)-(d) show the Δm distributions. In Fig. 1(d) the peak is broadened because of the missing π^0 meson. Also shown by the shaded histograms are the spectra from the "wrong sign" low-energy pion ($D^0\pi^-$) combinations. We define the signal region as follows. The two fully reconstructed modes use the Δm range 0.144 to 0.147 GeV/c^2, and the $K^-\pi^+\pi^0$ mode uses the range $\Delta m < 0.155$ GeV/c^2. The numbers of events in the signal regions are 935, 1166, and 2858, respectively.

We estimate the numbers of combinatorial background events by using the shapes of the Δm spectra of the wrong sign ($D^0\pi^-$) combinations and normalizing them to the number of events in the Δm sideband. The estimated background fractions are 0.09 ± 0.01, 0.18 ± 0.02

and 0.37 ± 0.02, respectively. They are summarized in Table I.

It is possible that real D^0 or D^{*+} mesons are accompanied by a hadron h^- that was misidentified as a lepton, and such events can be included in the above samples. The hadrons can be either the decay products of the same B hadron that produced the charm meson or the primary particles produced in $\bar{p}p \to b\bar{b}X$ and $\bar{p}p \to c\bar{c}X$ events. We investigate this possibility by studying the wrong sign combinations, ℓ^+ with D^0 or D^{*+}, which cannot originate from B meson decays. We see no evidence for signal in these combinations. Based on this study we estimate the contribution of the $D^{(*)}h^-$ pairs to our signal to be $(1.2^{+2.4}_{-1.2})\%$, where possible charge correlations between the charm meson and the hadrons are considered. We ignore this background, and treat it as a systematic uncertainty.

IV. DECAY LENGTH MEASUREMENT AND MOMENTUM ESTIMATE

A schematic representation of the B meson semileptonic decay topology is illustrated in Fig. 2. The B meson decay vertex $\vec{V}_B$ is obtained by intersecting the trajectory of the lepton track with the flight path of the D^0 candidate. The B decay length L_B is defined as the displacement of $\vec{V}_B$ from the primary vertex $\vec{V}_P$, measured in the plane perpendicular to the beam axis, and projected onto the transverse momentum vector of the lepton-D^0 system:

$$L_B \equiv \frac{(\vec{V}_B - \vec{V}_P) \cdot \vec{p}_T^{\,\ell^- D^0}}{p_T^{\ell^- D^0}}.$$

To measure a proper decay length of a B meson decay, we need to know the momentum of the B meson. In semileptonic decays, the B meson momentum cannot be measured precisely because of the missing neutrino. We use $p_T^{\ell^- D^0}$ to estimate the B momentum for each event, which results in a corrected decay length defined as

$$x = L_B \, m_B / p_T^{\ell^- D^0}.$$

We call it the 'pseudo-proper decay length'. The residual correction between $p_T^{\ell^- D^0}$ and p_T^B is performed during lifetime fits we shall describe later.

A typical resolution on this decay length x due to vertex determination is 50 μm, including the contribution from the finite size of the primary vertex. For subsequent lifetime

measurements, we use only those events in which the resolutions on reconstructed decay lengths x are smaller than 0.05 cm. Also we require the proper decay length of the D^0 meson, measured from the B meson decay vertex to the D^0 decay vertex, to be in the range from -0.1 cm to 0.1 cm with its uncertainty smaller than 0.05 cm. These cuts reject poorly measured decays and reduce random track combinations. In addition, we limit ourselves to events with reconstructed decay lengths x in the range between -0.15 cm and 0.3 cm. These cuts have been applied already for the charm signals shown in Fig. 1.

As mentioned above, we have used the momentum of the lepton-D^0 system, $p_T^{\ell^- D^0}$, to calculate the pseudo-proper decay length. However, we still need to account for the missing momentum to measure B meson lifetimes. We define the ratio K of the observed momentum to the true momentum as

$$K = p_T^{\ell^- D^0} / p_T^B.$$

The K distribution is obtained from a Monte Carlo calculation. The ISAJET event generator [14] is used for the production of the b quark, where the shape of the p_T spectrum is modified slightly to match the QCD calculation in the next-to-leading order [15]. The fragmentation model by Peterson and others [16] is used. The CLEO event generator [17] is used to describe B meson decays. In particular, the semileptonic decays adopt the model by Isgur and others (ISGW) [18]. A typical K distribution thus obtained has an average value of 0.85 with an rms width of 0.11, and is approximately independent of the $p_T^{\ell^- D^0}$ in the range of interest, which is typically 15 to 25 GeV/c. It is also independent of the D^0 decay mode except for the partially reconstructed mode $D^0 \to K^-\pi^+\pi^0$, which has a slightly lower mean value (about 0.80) because of the missing π^0 particle. Two K distributions are shown in Fig. 3.

The lifetime is determined from a maximum likelihood fit to the observed pseudo-proper decay length distributions. The likelihood for the signal sample is given by

$$\mathcal{L}_{\rm SIG} = \prod_i [(1 - f_{\rm BG})\mathcal{F}_{\rm SIG}(x_i) + f_{\rm BG}\mathcal{F}_{\rm BG}(x_i)],$$

where x_i is the pseudo-proper decay length measured for event i, and the product is taken over observed events in the sample. The first term in the likelihood function represents a

B decay signal event, while the second term accounts for combinatorial background events whose fraction in the sample is $f_{\rm BG}$. The signal probability density function $\mathcal{F}_{\rm SIG}(x)$ consists of an exponential decay function $\frac{K}{c\tau}\exp(-\frac{Kx}{c\tau})$ defined for positive decay lengths, smeared with a normalized K distribution $D(K)$ and a Gaussian distribution with width $s\sigma_i$:

$$\mathcal{F}_{\rm SIG}(x) = \int dK\, D(K)\, \left[\theta(x)\,\frac{K}{c\tau}\exp\left(-\frac{Kx}{c\tau}\right) \otimes G(x)\right],$$

where τ is the B meson lifetime, c is the speed of light, $\theta(x)$ is the step function defined as $\theta(x) = 1$ for $x \geq 0$ and $\theta(x) = 0$ for $x < 0$, and the symbol "$\otimes$" denotes a convolution. $G(x)$ is the Gaussian distribution given by

$$G(x) = \frac{1}{s\sigma_i\sqrt{2\pi}}\,\exp\left(-\frac{x^2}{2s^2\sigma_i^2}\right),$$

and σ_i is the estimated resolution on x_i. The scale factor s is introduced as a fit parameter and accounts for a possible incompleteness of our estimate of the decay length resolution. The integration over the momentum ratio K is approximated by a finite sum

$$\int dK\, D(K) \rightarrow \sum_j D(K_j)\Delta K,$$

where the sum is taken over bin j of a histogrammed distribution $D(K_j)$ with bin width ΔK.

The pseudo-proper decay length distribution of combinatorial background events, $\mathcal{F}_{\rm BG}(x)$, is measured using mass sideband events, assuming that they represent the combinatorial background events under signal mass peaks. The functional form of the distribution is parameterized empirically by a sum of a Gaussian distribution centered at zero, and positive and negative exponential tails smeared with a Gaussian distribution:

$$\begin{aligned}\mathcal{F}_{\rm BG}(x) = {} & (1 - f_- - f_+)\, G(x) \\ & + (f_+/\lambda_+)\,\theta(x)\exp(-x/\lambda_+) \otimes G(x) \\ & + (f_-/\lambda_-)\,\theta(-x)\exp(+x/\lambda_-) \otimes G(x).\end{aligned}$$

The shape of the background function (parameters $f_\pm$ and $\lambda_\pm$) and the resolution scale factor s, as well as the signal lifetime $c\tau$, are determined from a simultaneous fit to a signal sample

and a background sample. We use the combined likelihood $\mathcal{L}$ defined as $\mathcal{L} = \mathcal{L}_{\rm SIG}\ \mathcal{L}_{\rm BG}$, where $\mathcal{L}_{\rm BG} = \prod_k \mathcal{F}_{\rm BG}(x_k)$ and the product is taken over event k in the background sample. The amount of combinatorial background $f_{\rm BG}$ is also a parameter in the simultaneous fit. This parameter is constrained by adding a term $\frac{1}{2}\chi^2 = \frac{1}{2}(f_{\rm BG} - \langle f_{\rm BG}\rangle)^2/\sigma^2_{\rm BG}$ to the negative log-likelihood $-\ell = -\ln\mathcal{L}$. The average background fraction $\langle f_{\rm BG}\rangle$ and its uncertainty $\sigma_{\rm BG}$ are estimated from the signal mass distributions (Table I).

The background sample for the $\ell^- D^0$ mode is formed from the D^0 sidebands, defined by the mass ranges 1.74 to 1.79 and 1.94 to 1.99 GeV/c^2. For the $\ell^- D^{*+}$ samples we use Δm sidebands: we use the right sign $(D^0\pi^+)$ sideband $0.15 < \Delta m < 0.19$ GeV/c^2 for the two fully reconstructed D^0 modes, and $0.16 < \Delta m < 0.19$ GeV/c^2 for the $D^0 \to K^-\pi^+\pi^0$ mode. The background samples are summarized in Table II.

The pseudo-proper decay length distributions of the background samples are shown in Fig. 4, together with fit results. The background parameter values and the resolution scale s determined from the fit are listed in Table III. The corresponding decay length distributions of the signal samples are shown in Fig. 5. We find the lifetimes to be $c\tau(B) = 489 \pm 15, 462 \pm 18, 472 \pm 19$ and 449 ± 14 μm for the four modes, where uncertainties are statistical only.

As a check of the procedure, we measure the D^0 lifetime using the proper decay length measured from the secondary vertex $\vec{V}_B$ to the D^0 decay vertex. The proper decay length distributions are shown in Fig. 6, together with fit results. The lifetime numbers are summarized in Table IV. The result is in reasonably good agreement with the world average value of 124.4 ± 1.2 μm [19].

V. B^- AND $\overline{B}^0$ MESON LIFETIMES

In order to extract the B^- and $\overline{B}^0$ meson lifetimes, we must take into account the fact that the $\ell^- D^0$ and $\ell^- D^{*+}$ samples are admixtures of the two B meson decays. The semileptonic decays can be expressed as $\overline{B} \to \ell^-\overline{\nu}\mathbf{D}$, where $\mathbf{D}$ is a charm system whose charge is correlated with the B meson charge. If only the two lowest mass charm states, pseudoscalar (D) and vector (D^*), are produced, the $\ell^- D^{*+}$ combination can arise only

from the $\overline{B}^0$ meson decay. Similarly, the $\ell^- D^0$ combination comes only from B^- meson decays, provided that the D^0 from the D^{*+} decay is excluded. However, it is known that the above two states do not saturate the total semileptonic decay rates. All data indicate that higher mass charm mesons, D^{**} states, as well as non-resonant $D^{(*)}\pi$ pairs, are responsible for the rest of the semileptonic decays. We do not distinguish resonant and non-resonant components, and refer to both of them as D^{**}.

These D^{**} meson decays can dilute the charge correlation between the observed final states and the parent B meson. For example, the D^{**0} meson decays to $D^{(*)+}\pi^-$ as well as $D^{(*)0}\pi^0$ final states, resulting in misidentification of B^- meson decays as $\overline{B}^0 \to D^{*+}\ell^-\bar{\nu}X$. Nevertheless, $\ell^- D^0$ and $\ell^- D^{*+}$ combinations are dominated by B^- and $\overline{B}^0$ meson decays, respectively. As described below, the contamination of the wrong B meson species is only at 10-15% level. This enable us to extract the two B meson lifetimes.

A. Sample composition

We estimate the fraction of B^- decays g^- in the $\ell^- D^0$ and $\ell^- D^{*+}$ samples as follows. The production rates of charged and neutral B mesons and their semileptonic decay widths are assumed to be equal. We also assume the D^{**} meson decays exclusively to $D^{(*)}\pi$ via the strong interaction, thereby allowing us to determine the branching fractions, e.g. $D^{(*)+}\pi^0$ vs $D^{(*)0}\pi^+$, using isospin symmetry. We consider four factors affecting the composition. First, the composition depends on the fraction (f^{**}) of the D^{**} mesons produced in semileptonic B decays,

$$f^{**} = \frac{\mathcal{B}(\overline{B} \to \ell^-\bar{\nu}D^{**})}{\mathcal{B}(\overline{B} \to \ell^-\bar{\nu}DX)} = 1 - \frac{\mathcal{B}(\overline{B} \to \ell^-\bar{\nu}D) + \mathcal{B}(\overline{B} \to \ell^-\bar{\nu}D^*)}{\mathcal{B}(\overline{B} \to \ell^-\bar{\nu}DX)}.$$

The CLEO experiment measures the fraction of exclusive decays to the two lowest mass states to be $0.64 \pm 0.10 \pm 0.06$ [20]. Thus, we find that $f^{**} = 0.36 \pm 0.12$. A few experiments have recently observed some D^{**} modes [21], but the sum of exclusive modes still does not add up to the total semileptonic rate. Second, g^- depends on the relative abundance of various possible D^{**} states, because some of them decay only to $D^*\pi$ and others to $D\pi$, depending on the spin and parity. This relative abundance is not measured very well at

present. Changing the abundance is equivalent to changing the branching fractions for $D^*\pi$ and $D\pi$ averaged over various D^{**} states. We define a quantity P_V as

$$P_V = \frac{\mathcal{B}(D^{**} \to D^*\pi)}{\mathcal{B}(D^{**} \to D^*\pi) + \mathcal{B}(D^{**} \to D\pi)},$$

where $\mathcal{B}$ denotes a branching fraction. We assume the relative abundance predicted in Ref. [18], which corresponds to $P_V = 0.78$. We also consider the extreme values $P_V = 0.0$ and 1.0. Third, the composition depends on the ratio of the B^- and $\overline{B}^0$ meson lifetimes, because the number of $\ell^- D^{(*)}$ events is proportional to the semileptonic branching fraction, which is the product of the lifetime and the semileptonic partial width. Finally, the sample composition depends on the reconstruction efficiency of the low energy pion in the decay $D^{*+} \to D^0\pi^+$. If we miss the pion and reconstruct the D^0 meson, the D^{*+} decay is included in the $\ell^- D^0$ sample and the sample composition is altered. The efficiency is measured to be $\epsilon(\pi) = 0.93^{+0.07}_{-0.21}$ by studying the rates of $\ell^- D^{*+}$ events with respect to $\ell^- D^0$ events.

We also have to take into account the differences in the reconstruction efficiencies for the $\overline{B} \to \ell^- \bar{\nu} D$, D^* and D^{**} decay modes. We examine this effect by using the Monte Carlo events we have used to obtain the K distributions. The ISGW model was used for semileptonic decays. We find that the first two modes show very similar efficiencies, while the last mode has an efficiency that is lower by about a factor of two.

The dependence of the B^- fraction g^- on the parameters f^{**} and P_V are illustrated in Figs. 7 and 8. We find that $g^- = 0.85^{+0.05}_{-0.12}$ for the $\ell^- D^0$ sample and $g^- = 0.10^{+0.09}_{-0.10}$ for the $\ell^- D^{*+}$ sample when the two lifetimes are identical. The central values correspond to the nominal choice of the parameters, $f^{**} = 0.36$, $P_V = 0.78$ and $\epsilon(\pi) = 0.93$. The uncertainties reflect maximum changes in g^- when the three parameters are changed within their uncertainties, namely f^{**} to 0.24 and 0.48, P_V to 0.0 and 1.0, and $\epsilon(\pi)$ to 0.72 and 1.0.

We also note that the momentum correction factors (K distributions) need to be modified when the sample composition parameters are changed. The K distributions for the decay $\overline{B} \to \ell^- \bar{\nu} D^{**}$ have lower mean values because of additional missing particle(s), and changing the amount of D^{**} decays results in changes in the K distributions.

There are other physics processes that can produce the lepton-$D^{(*)}$ signature. The largest background comes from the decay of the $\overline{B}^0_s$ meson, $\overline{B}^0_s \to \ell^- \overline{\nu} D_s^{**+}$, followed by $D_s^{**+} \to$

$D^{(*)}K$. The contribution of this process to the lepton-$D^{(*)}$ signal is estimated to be about 2%. Other processes such as $\overline{B} \to \tau^- \bar{\nu}_\tau D^{(*)} X$ followed by $\tau^- \to \ell^- \bar{\nu}_\ell \nu_\tau$, and $\overline{B} \to D_s^- D^{(*)} X$ followed by $D_s^- \to \ell^- X$, are suppressed severely because of branching fractions and kinematic requirements on leptons. We have ignored these backgrounds here. Therefore the fraction of $\overline{B}^0$ mesons is given by $g^0 = 1 - g^-$. We treat effects of the physics backgrounds as a systematic uncertainty.

B. Lifetime fit

We can now determine the B^- and $\overline{B}^0$ lifetimes with a combined fit of the $\ell^- D^0$ and $\ell^- D^{*+}$ samples. The likelihood is given by

$$\mathcal{L} = \prod_{\text{sample}} \left\{ \prod_i [\,(1 - f_{\rm BG})\mathcal{F}_{\rm SIG}(x_i) + f_{\rm BG}\mathcal{F}_{\rm BG}(x_i)\,] \prod_k \mathcal{F}_{\rm BG}(x_k) \right\},$$

where the product is taken over event i in each signal sample, event k in each background sample, and over the $\ell^- D^0$ and $\ell^- D^{*+}$ samples. For each signal sample, we use a two-component signal distribution function given by

$$\mathcal{F}_{\rm SIG}(x) = g^- \mathcal{F}^-_{\rm SIG}(x) + (1 - g^-)\mathcal{F}^0_{\rm SIG}(x),$$

where $\mathcal{F}^-_{\rm SIG}(x)$ and $\mathcal{F}^0_{\rm SIG}(x)$ represent the B^- and $\overline{B}^0$ meson components, respectively. The dependence of g^- on the lifetime ratio is taken into account during lifetime fits.

The result of the combined fit is $c\tau(B^-) = 491 \pm 17$ μm, $c\tau(\overline{B}^0) = 442 \pm 12$ μm, where the quoted uncertainties are statistical, and are correlated with each other with a coefficient of -0.308. From these numbers we calculate the ratio of the lifetimes to be $\tau(B^-)/\tau(\overline{B}^0) = 1.110 \pm 0.056$.

The pseudo-proper decay length distributions of the $\ell^- D^0$ sample and the combined $\ell^- D^{*+}$ sample are shown in Figs. 9 and 10. The results of the combined fit are superimposed.

C. Systematic uncertainties

The sample composition is a source of systematic uncertainty in the B meson lifetime determination. We change each one of the parameters f^{**}, P_V and $\epsilon(\pi)$ to another value

while keeping others at their nominal values, compute the sample composition g^- and fit for the two B meson lifetimes. The results are listed in Table V. We interpret the observed changes as systematic uncertainties.

Other sources of systematic uncertainties considered in this analysis are described below. They are summarized in Table VI.

We have estimated the decay length distributions from real data using mass sidebands, thus minimizing model dependence. However, the assumed functional form may not be fully adequate to describe the true shapes. Thus, we have considered an alternative parameterization that includes additional exponential terms; this has turned out to give only minimal changes in the result.

Physics and fake lepton background processes are studied by adding their simulated decay length distributions to the background function.

Other sources of systematic uncertainties include our estimate of the decay length resolution and of the B meson momentum. We have introduced a resolution scale factor s and find a value of about 1.35. We change this factor to 1.0 or 1.7, fix it at the value and repeat the lifetime fitting procedure. We assign the observed changes as an uncertainty. The momentum correction (K distribution) is subject to some uncertainty too, because it depends on the kinematics of B meson production and of semileptonic decays. An alternative p_T spectral shape of the b quark production was considered, based on a comparison of lepton p_T shape in the real data and Monte Carlo events. A simple $V-A$ decay model was tried in place of the ISGW model to describe semileptonic decays. We apply these changes and obtain new K distributions, and repeat the lifetime fits. The observed changes are listed as a systematic uncertainty. In addition, the K distributions are somewhat dependent on the lepton momentum and on the cuts used for electron identification. We assign uncertainties due to possible incompleteness in the treatment of these effects. As stated earlier, the momentum correction depends on the assumed amount of B decays to D^{**} mesons. This effect is already accounted for in the sample composition uncertainty.

Also, we have applied a loose cut on the D^0 decay length in some modes, and it introduces a slight bias (about 2.5 μm) toward a longer lifetime. Here we quote the number without

correction to the final lifetimes and assign a systematic uncertainty. Finally, a possible residual misalignment of the SVX detector and the stability of the position of the Tevatron beam are considered. Some of these uncertainties are common to the two B mesons and cancel in the determination of the lifetime ratio. All these effects are combined in quadrature to give the total systematic uncertainty.

VI. FINAL RESULTS AND CONCLUSION

We have measured the lifetimes of the B^- and $\overline{B}^0$ mesons using their partially reconstructed semileptonic decays $\overline{B} \to \ell^- \overline{\nu} D^0 X$ and $\overline{B} \to \ell^- \overline{\nu} D^{*+} X$. Our final results are

$$\begin{aligned}
\tau(B^-) &= 1.637 \pm 0.058 \,^{+\,0.045}_{-\,0.043} \text{ ps}, \\
\tau(\overline{B}^0) &= 1.474 \pm 0.039 \,^{+\,0.052}_{-\,0.051} \text{ ps}, \\
\tau(B^-)/\tau(\overline{B}^0) &= 1.110 \pm 0.056 \,^{+\,0.033}_{-\,0.030},
\end{aligned}$$

where the first uncertainties are statistical and the second are systematic. The result is consistent with other recent measurements [3,5]. We combine this measurement with the CDF measurement [5] using fully reconstructed decays,

$$\begin{aligned}
\tau(B^-) &= 1.68 \pm 0.07 \pm 0.02 \text{ ps}, \\
\tau(\overline{B}^0) &= 1.58 \pm 0.09 \pm 0.02 \text{ ps}, \\
\tau(B^-)/\tau(\overline{B}^0) &= 1.06 \pm 0.07 \pm 0.02,
\end{aligned}$$

and derive the following CDF average:

$$\begin{aligned}
\tau(B^-) &= 1.661 \pm 0.052 \text{ ps}, \\
\tau(\overline{B}^0) &= 1.513 \pm 0.053 \text{ ps}, \\
\tau(B^-)/\tau(\overline{B}^0) &= 1.091 \pm 0.050,
\end{aligned}$$

where the uncertainties include both statistical and systematic effects. There exists a small (about 3 μm) correlation in systematic effects between the two measurements, such as due to detector alignment, and it is taken into account in combining the results.

The ratio of the two B meson lifetimes differs from unity by about 9%, or two standard deviations. This agrees with the small difference predicted by theory. The result is also consistent with the current world average value of 1.03 ± 0.05 [19]. The $\overline{B}^0$ meson lifetime is consistent with the $\overline{B}_s^0$ meson lifetime [22] within the uncertainty.

ACKNOWLEDGMENTS

We thank the Fermilab staff and the technical staffs of the participating institutions for their vital contributions. This work was supported by the U.S. Department of Energy and National Science Foundation; the Italian Istituto Nazionale di Fisica Nucleare; the Ministry of Education, Science and Culture of Japan; the Natural Sciences and Engineering Research Council of Canada; the National Science Council of the Republic of China; the A. P. Sloan Foundation; the Swiss National Science Foundation.

REFERENCES

[1] M. B. Voloshin and M. A. Shifman, Sov. Phys. JETP **64**, 698 (1986); I. I. Bigi *et al.*, in *B Decays, 2nd ed.*, S. Stone (ed.) (World Scientific, Singapore, 1994); G. Bellini, I. I. Bigi and P. J. Dornan, Phys. Rep. **289**, 1 (1997).

[2] M. Neubert and C. T. Sachrajda, Nucl. Phys. B **483**, 339 (1997).

[3] ALEPH Collaboration, D. Buskulic *et al.,* Z. Phys. C **71**, 31 (1996); DELPHI Collaboration, P. Abreu *et al.,* Z. Phys. C **68**, 13 (1995); DELPHI Collaboration, W. Adam *et al.,* Z. Phys. C **68**, 363 (1995); DELPHI Collaboration, P. Abreu *et al.,* Z. Phys. C **74**, 19 (1997); OPAL Collaboration, R. Akers *et al.,* Z. Phys. C **67**, 379 (1995); SLD Collaboration, K. Abe *et al.,* Phys. Rev. Lett. **79**, 590 (1997).

[4] CDF Collaboration, F. Abe *et al.,* Phys. Rev. Lett. **76**, 4462 (1996).

[5] CDF Collaboration, F. Abe *et al.,* Phys. Rev. D **57**, 5382 (1998).

[6] CLEO Collaboration, M. Athanas *et al.,* Phys. Rev. Lett. **73**, 3503 (1994); **74**, 3090(E) (1995).

[7] CDF Collaboration, F. Abe *et al.,* Nucl. Instrum. Methods Phys. Res. A **271**, 387 (1988), and references therein.

[8] In CDF, φ is the azimuthal angle, θ is the polar angle measured from the proton direction, and r is the radius from the beam axis (z-axis).

[9] D. Amidei *et al.,* Nucl. Instrum. Methods Phys. Res. A **350**, 73 (1994); P. Azzi *et al.,* Nucl. Instrum. Methods Phys. Res. A **360**, 137 (1995).

[10] K. Byrum *et al.,* Nucl. Instrum. Methods Phys. Res. A **364**, 144 (1995).

[11] CDF Collaboration, F. Abe *et al.,* Phys. Rev. D **52**, 2624 (1995).

[12] CDF Collaboration, F. Abe *et al.,* Phys. Rev. Lett. **68**, 2734 (1992); CDF Collaboration, F. Abe *et al.,* Phys. Rev. D **48**, 2998 (1993).

[13] CDF Collaboration, F. Abe *et al.,* Phys. Rev. Lett. **71**, 3421 (1993).

[14] F. E. Paige and S. D. Protopopescu, Report No. BNL-38034, 1986 (unpublished).

[15] P. Nason, S. Dawson and R. K. Ellis, Nucl. Phys. B **327**, 49 (1989).

[16] C. Peterson, D. Schlatter, I. Schmitt, and P. M. Zerwas, Phys. Rev. D **27**, 105 (1983).

[17] P. Avery, K. Read, and G. Trahern, Report No. CSN-212, 1985 (unpublished).

[18] N. Isgur, D. Scora, B. Grinstein, and M. Wise, Phys. Rev. D **39**, 799 (1989).

[19] R. M. Barnett *et al.*, Phys. Rev. D **54**, 1 (1996), and 1997 partial update available at http://pdg.lbl.gov.

[20] CLEO Collaboration, R. Fulton *et al.*, Phys. Rev. D **43**, 651 (1991).

[21] ALEPH Collaboration, D. Busklic *et al.*, Phys. Lett. B **345**, 103 (1995); ALEPH Collaboration, D. Busklic *et al.*, Z. Phys. C **73**, 601 (1997); DELPHI Collaboration, P. Abreu *et al.*, Z. Phys. C **71**, 539 (1996); OPAL Collaboration, R. Akers *et al.*, Z. Phys. C **67**, 57 (1995); CLEO Collaboration, A. Anastassov *et al.*, Report No. CLEO 97-17, January (1998), submitted to Phys. Rev. Lett.

[22] CDF Collaboration, F. Abe *et al.*, Phys. Rev. Lett. **74**, 4988 (1995); CDF Collaboration, F. Abe *et al.*, Phys. Rev. Lett. **77**, 1945 (1996); ALEPH Collaboration, D. Buskulic *et al.,* Phys. Lett. B **377**, 205 (1996); ALEPH Collaboration, D. Buskulic *et al.,* Z. Phys. C **69**, 585 (1996); DELPHI Collaboration, P. Abreu *et al.,* Z. Phys. C **61**, 407 (1994); DELPHI Collaboration, P. Abreu *et al.,* Z. Phys. C **71**, 11 (1996); OPAL Collaboration, R. Akers *et al.,* Phys. Lett. B **350**, 273 (1995).

TABLES

B Mode	D^0 mode	D^0 mass range (GeV/c^2)	Δm range (GeV/c^2)	Events	Background fraction
$\ell^- D^0$	$K^-\pi^+$	1.84 – 1.88	Not D^{*+}	5198	0.526 ± 0.018
$\ell^- D^{*+}$	$K^-\pi^+$	1.83 – 1.90	0.144 – 0.147	935	0.086 ± 0.011
$\ell^- D^{*+}$	$K^-\pi^+\pi^+\pi^-$	1.84 – 1.88	0.144 – 0.147	1166	0.183 ± 0.015
$\ell^- D^{*+}$	$K^-\pi^+\pi^0$	1.50 – 1.70	< 0.155	2858	0.366 ± 0.016

TABLE I. Definition of signal samples, numbers of candidates and estimated background fraction.

B Mode	D^0 mode	D^0 mass range (GeV/c^2)	Δm range (GeV/c^2)	Events
$\ell^- D^0$	$K^-\pi^+$	1.74 – 1.79, 1.94 – 1.99	Not D^{*+}	7200
$\ell^- D^{*+}$	$K^-\pi^+$	1.83 – 1.90	0.15 – 0.19	1769
$\ell^- D^{*+}$	$K^-\pi^+\pi^+\pi^-$	1.84 – 1.88	0.15 – 0.19	5030
$\ell^- D^{*+}$	$K^-\pi^+\pi^0$	1.50 – 1.70	0.16 – 0.19	3809

TABLE II. Definition of background samples and numbers of events.

B Mode	D^0 mode	scale s	f_+	λ_+ (μm)	f_-	λ_- (μm)
$\ell^- D^0$	$K^-\pi^+$	1.38 ± 0.03	0.404 ± 0.008	531 ± 12	0.136 ± 0.007	240 ± 10
$\ell^- D^{*+}$	$K^-\pi^+$	1.32 ± 0.07	0.487 ± 0.017	498 ± 21	0.136 ± 0.014	240 ± 22
$\ell^- D^{*+}$	$K^-\pi^+\pi^+\pi^-$	1.38 ± 0.03	0.328 ± 0.011	362 ± 12	0.058 ± 0.008	216 ± 21
$\ell^- D^{*+}$	$K^-\pi^+\pi^0$	1.39 ± 0.04	0.536 ± 0.011	612 ± 17	0.098 ± 0.008	274 ± 20

TABLE III. Background shapes obtained from a simultaneous fit of signal and background samples.

B Mode	D^0 mode	$c\tau(B)$ (μm)	$c\tau(D^0)$ (μm)
$\ell^- D^0$	$K^-\pi^+$	489 ± 15	128.0 ± 5.3
$\ell^- D^{*+}$	$K^-\pi^+$	462 ± 18	133.8 ± 5.6
$\ell^- D^{*+}$	$K^-\pi^+\pi^+\pi^-$	472 ± 19	125.3 ± 5.2
$\ell^- D^{*+}$	$K^-\pi^+\pi^0$	449 ± 14	127.5 ± 5.0

TABLE IV. B and D^0 meson lifetimes measured for individual decay modes. Quoted uncertainties are statistical only.

f^{**}	P_V	$\epsilon(\pi)$	g^-		$c\tau$ (μm)		correl.	$\frac{\tau(B^-)}{\tau(\overline{B}^0)}$
			$\ell^- D^0$	$\ell^- D^{*+}$	B^-	$\overline{B}^0$	coeff.	
0.24	0.78	0.93	0.899	0.064	491.3 ± 16.3	448.0 ± 10.7	-0.187	1.097 ± 0.049
0.36	0.78	0.93	0.851	0.105	491.0 ± 17.3	442.2 ± 11.6	-0.308	1.110 ± 0.056
0.48	0.78	0.93	0.796	0.155	492.0 ± 18.9	434.2 ± 13.3	-0.461	1.133 ± 0.067
0.36	0.00	0.93	0.806	0.000	491.0 ± 17.5	448.2 ± 9.7	-0.105	1.096 ± 0.048
0.36	1.00	0.93	0.858	0.133	491.3 ± 17.4	440.2 ± 12.3	-0.360	1.116 ± 0.058
0.36	0.78	0.72	0.790	0.105	494.5 ± 18.7	441.7 ± 11.8	-0.357	1.120 ± 0.060
0.36	0.78	1.00	0.874	0.105	489.8 ± 16.8	442.3 ± 11.5	-0.290	1.107 ± 0.054

TABLE V. B^- and $\overline{B}^0$ lifetimes from a combined fit of $\ell^- D^0$ and $\ell^- D^{*+}$ samples under various sample composition conditions. Quoted uncertainties are statistical only and are correlated between B^- and $\overline{B}^0$. Also listed are their calculated ratios.

Source	Contribution to		
	$c\tau(B^-)$ (μm)	$c\tau(\overline{B}^0)$ (μm)	$\frac{\tau(B^-)}{\tau(\overline{B}^0)}$
Sample composition			
D^{**} fraction (f^{**})	$^{+1}_{-0}$	$^{+6}_{-8}$	$^{+0.023}_{-0.014}$
D^{**} composition (P_V)	$^{+1}_{-0}$	$^{+6}_{-2}$	$^{+0.006}_{-0.015}$
Low energy pion reconstruction	$^{+4}_{-1}$	± 1	$^{+0.009}_{-0.003}$
Background treatment	± 5	± 5	± 0.015
Decay length resolution	$^{+7}_{-5}$	$^{+7}_{-5}$	± 0.002
Momentum estimate			
b quark p_T spectrum	± 4	± 4	-
B decay model	± 4	± 4	-
Momentum dependence	± 6	± 6	-
Electron cuts	± 5	± 5	-
Decay length cut	$^{+0}_{-5}$	$^{+0}_{-5}$	± 0.016
Detector alignment	± 2	± 2	-
Total	± 13	$^{+16}_{-15}$	$^{+0.033}_{-0.030}$

TABLE VI. A summary of systematic uncertainties in the B^- and $\overline{B}^0$ lifetime measurement.

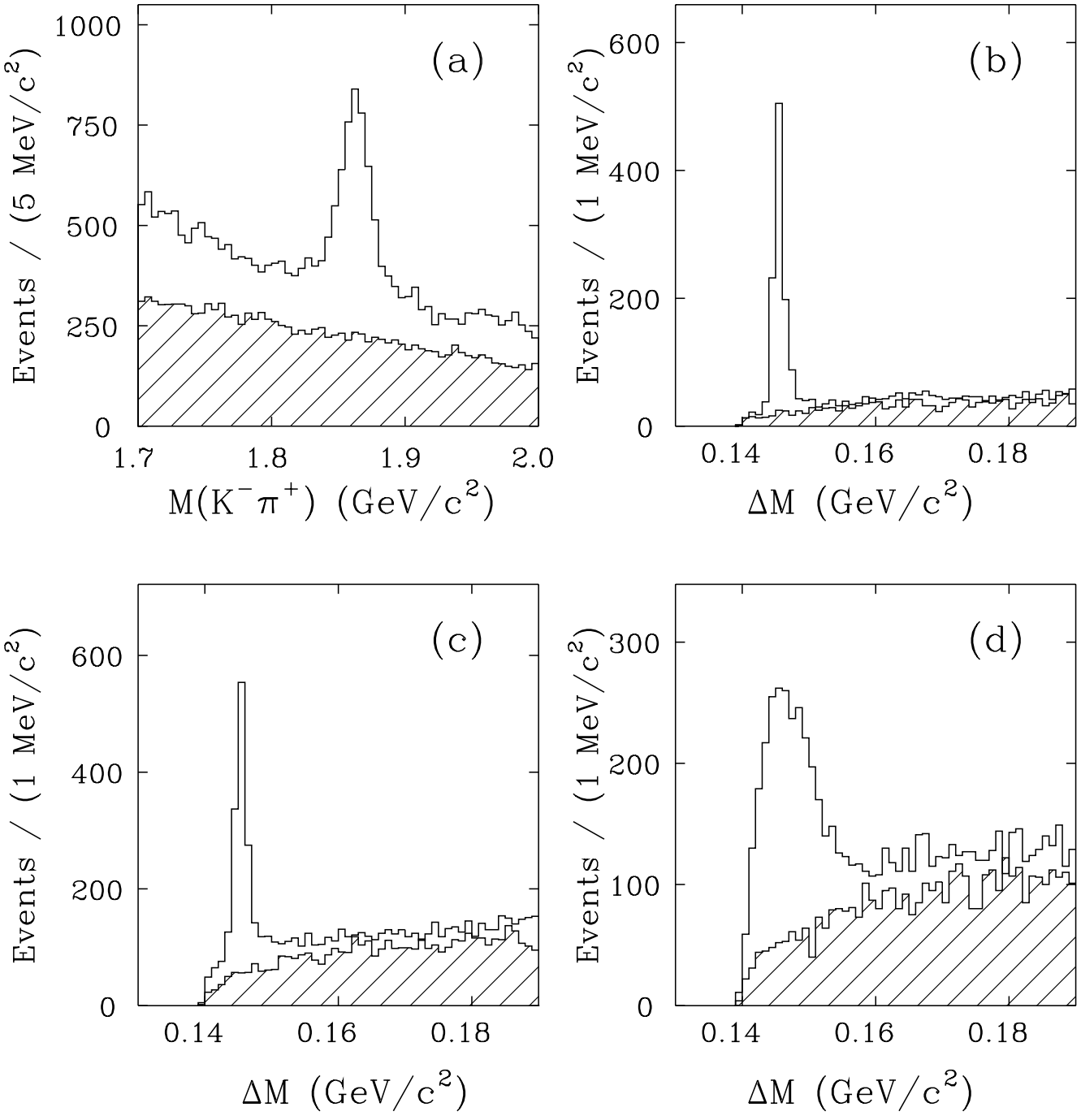

FIG. 1. Charm signals reconstructed in the vicinity of leptons ℓ^-. Four modes are shown: (a) $D^0 \to K^-\pi^+$ (non-D^{*+}), (b) $D^{*+} \to D^0\pi^+, D^0 \to K^-\pi^+$, (c) $D^{*+} \to D^0\pi^+, D^0 \to K^-\pi^+\pi^+\pi^-$ and (d) $D^{*+} \to D^0\pi^+, D^0 \to K^-\pi^+\pi^0$. Plot (a) shows the $K^-\pi^+$ invariant mass spectra, and (b-d) show the Δm distributions. Shaded histograms show wrong sign combinations, and in (a) they are scaled by 0.5 for display purposes.

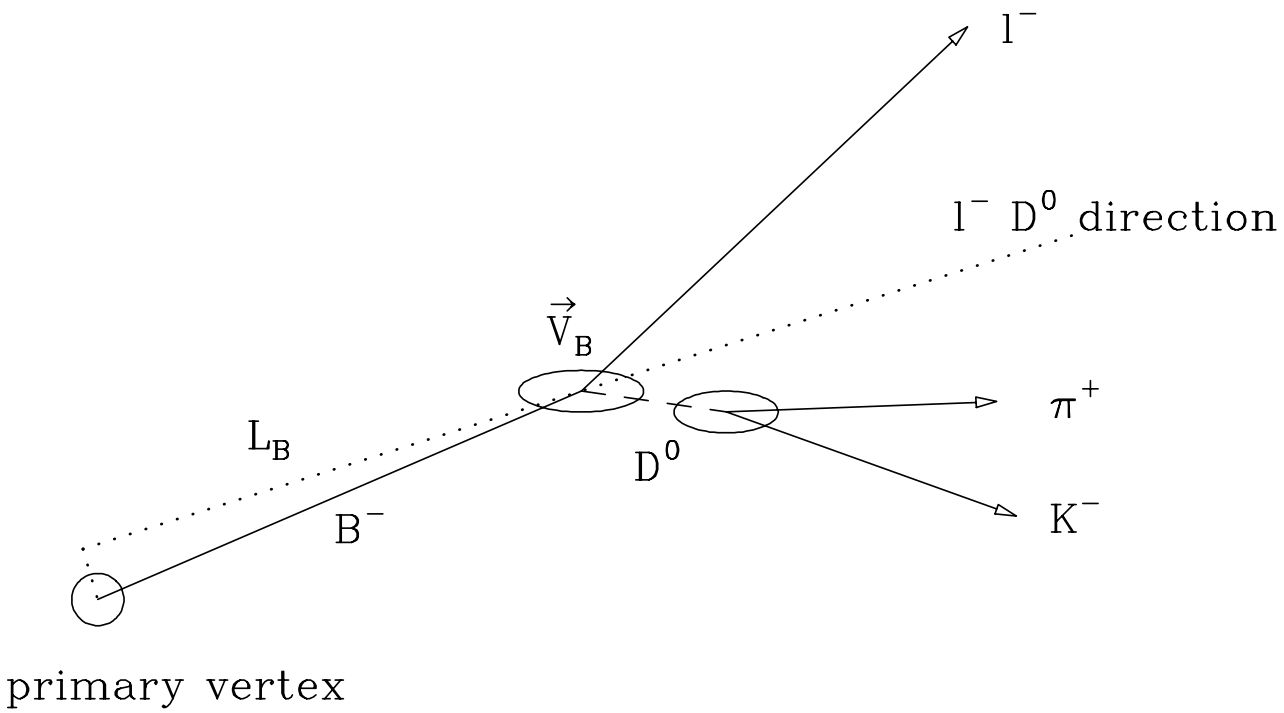

FIG. 2. Schematic representation of the decay $B^- \to \ell^- \bar{\nu} D^0 X$, $D^0 \to K^- \pi^+$.

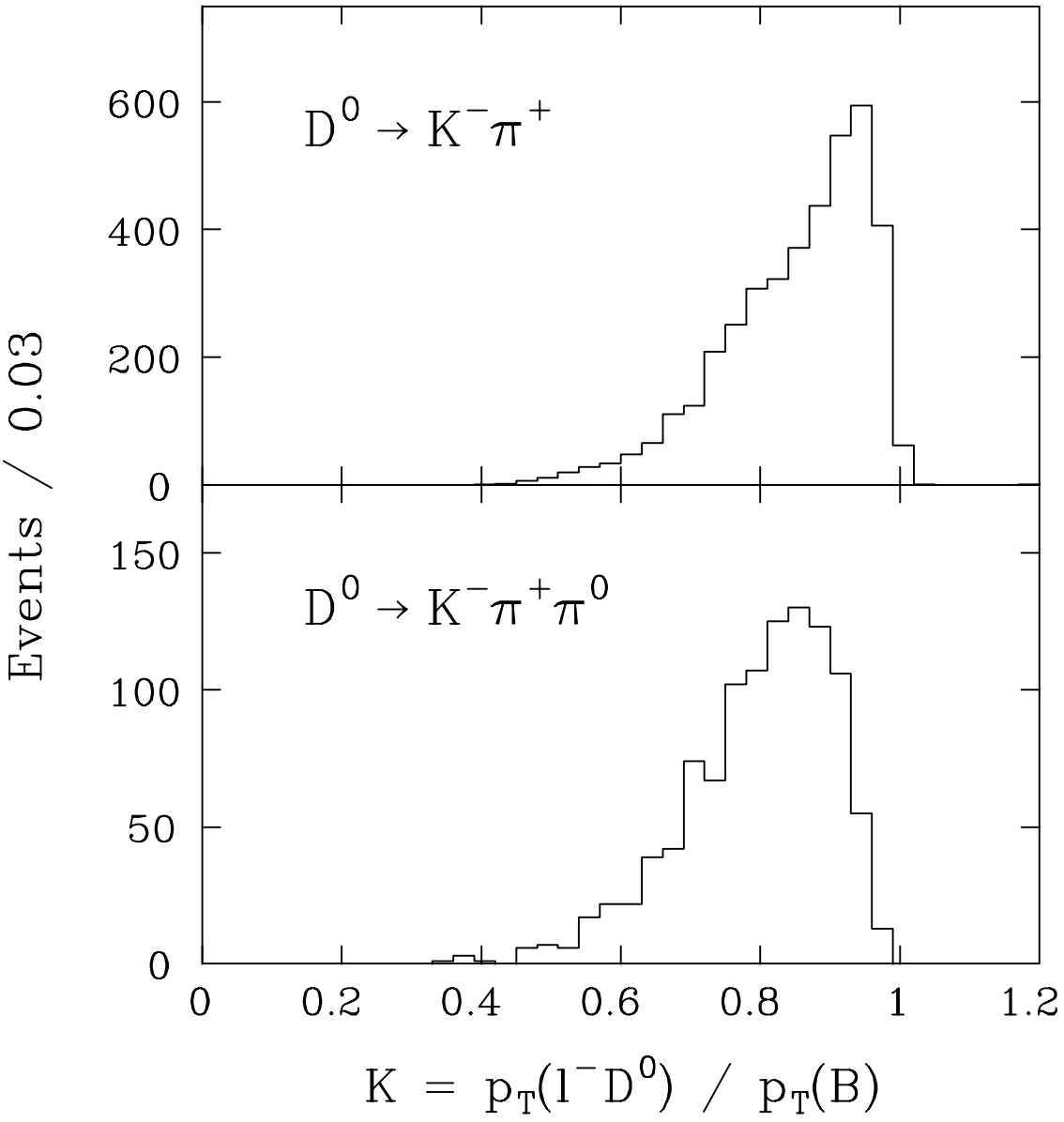

FIG. 3. Distribution of the momentum ratio K (see text) for $\overline{B} \to \ell^- \bar{\nu} D^0 X$, followed by $D^0 \to K^-\pi^+$ and $D^0 \to K^-\pi^+\pi^0$ decays obtained from a Monte Carlo calculation.

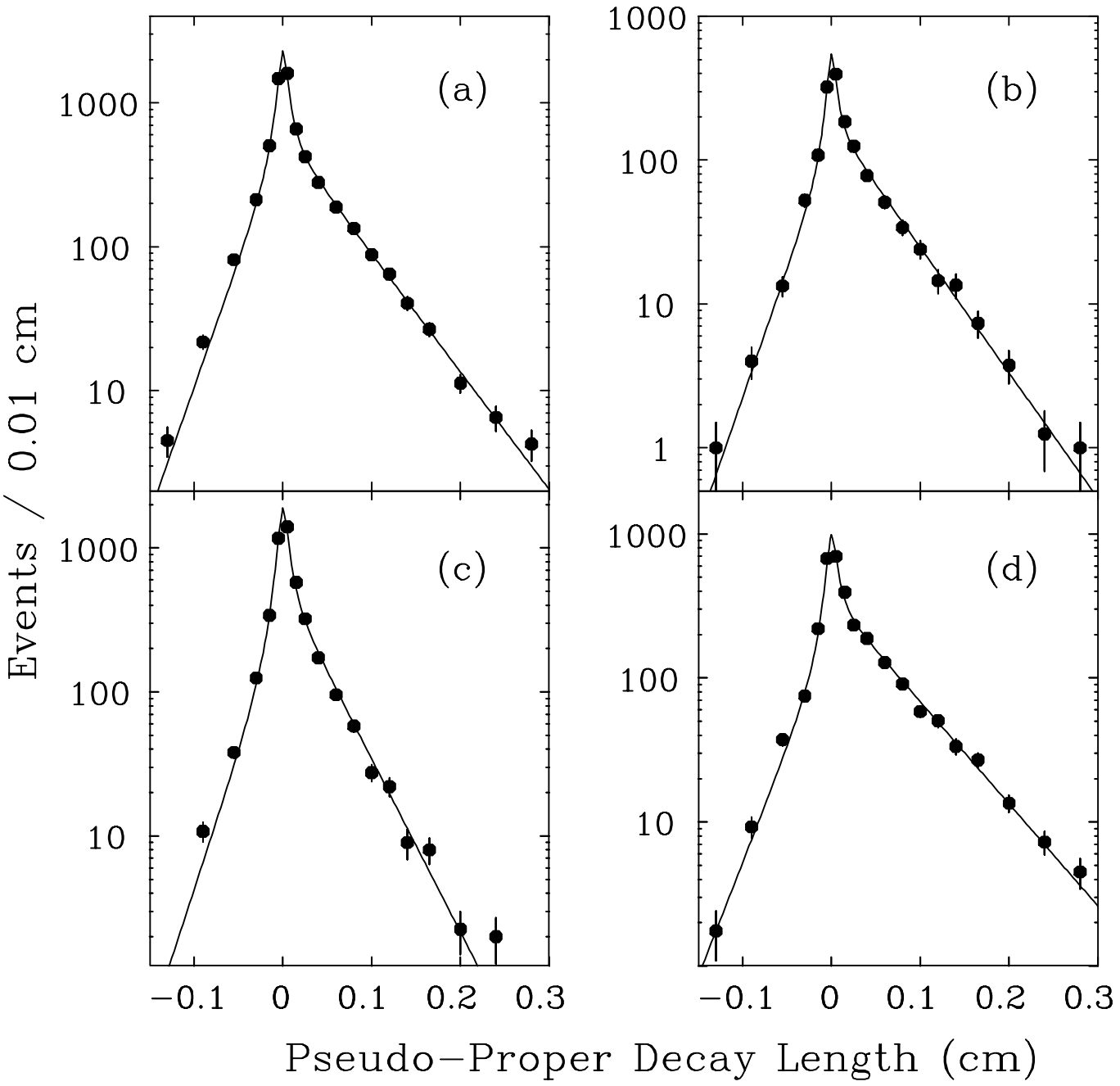

FIG. 4. Distributions of pseudo-proper decay lengths for lepton-D background samples (points). Also shown by the curve is the result of lifetime fits. Four decay modes are shown: (a) $\overline{B} \to \ell^- \bar{\nu} D^0 X$, $D^0 \to K^- \pi^+$ (non-D^{*+}), and $\overline{B} \to \ell^- \bar{\nu} D^{*+} X$, $D^{*+} \to D^0 \pi^+$, followed by (b) $D^0 \to K^- \pi^+$, (c) $D^0 \to K^- \pi^+ \pi^+ \pi^-$ and (d) $D^0 \to K^- \pi^+ \pi^0$.

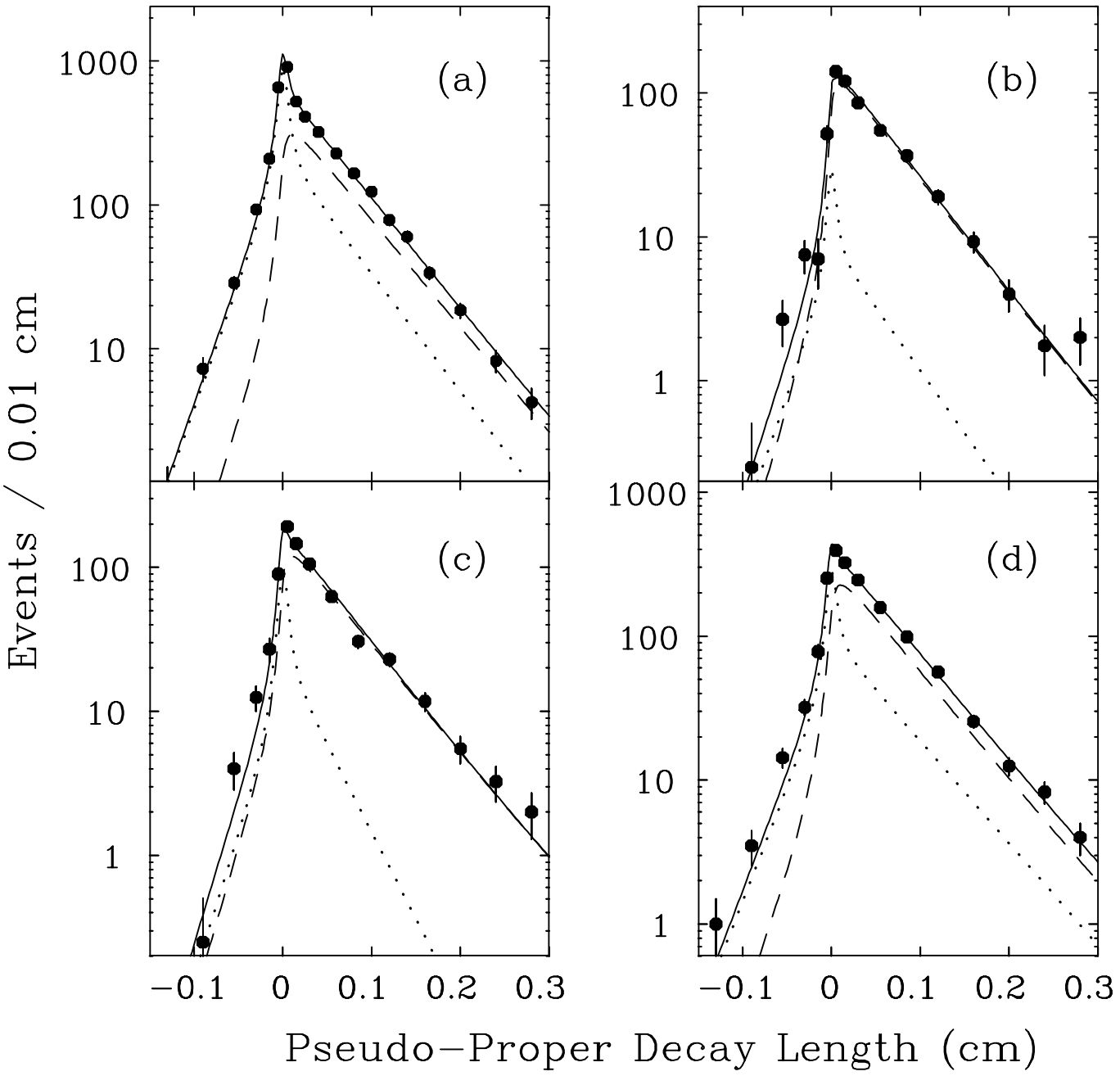

FIG. 5. Distributions of pseudo-proper decay lengths for lepton-D signal samples (points). Also shown are the result of lifetime fits, signal (dashed curve) and background (dotted curve) contributions, and the sum of the two (solid curve). The four decay modes (a-d) are the same as in Fig. 4.

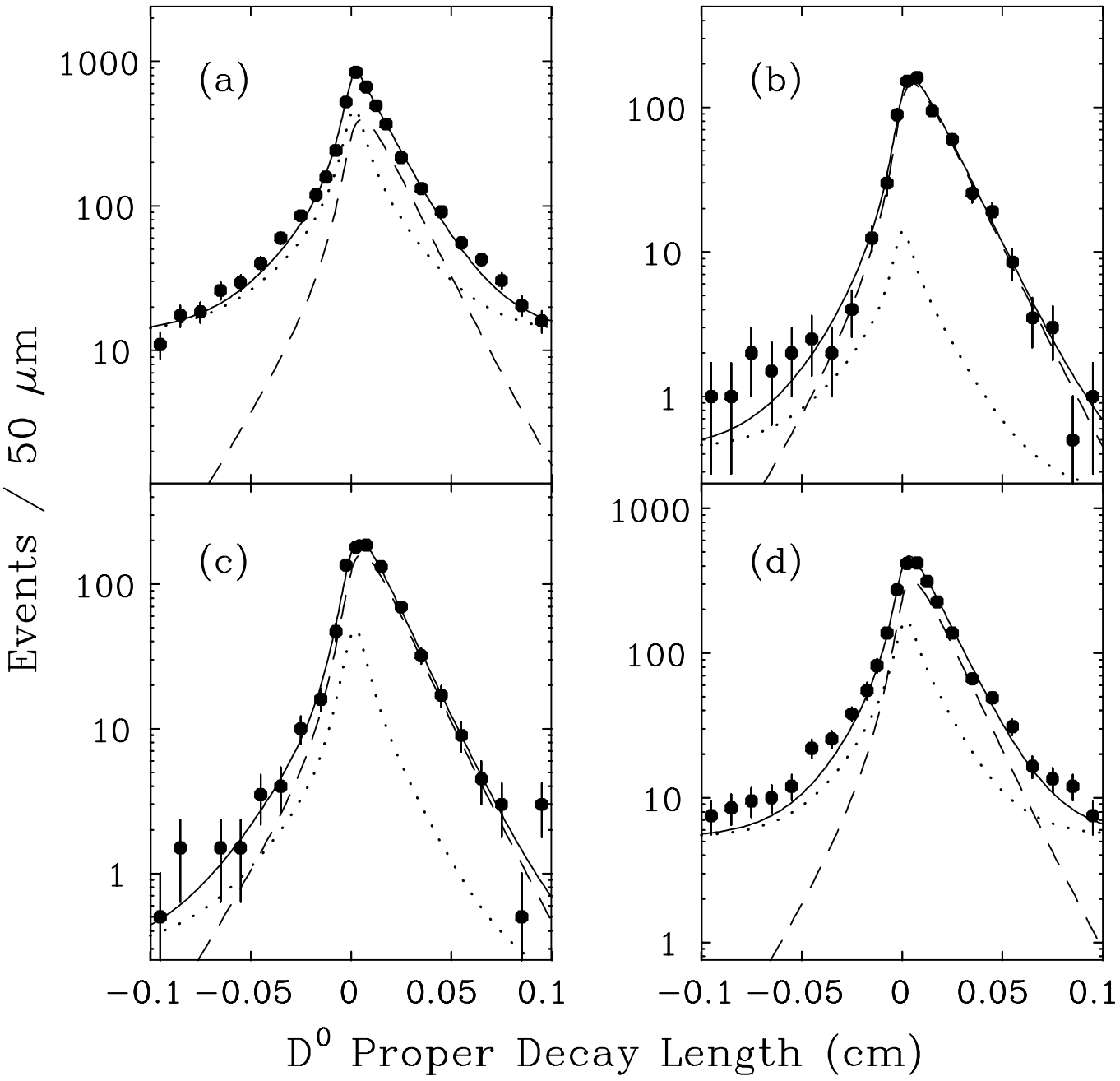

FIG. 6. Distributions of the D^0 proper decay lengths measured with respect to the B meson decay vertex (points). Also shown are the result of lifetime fits, signal (dashed curve) and background (dotted curve) contributions, and the sum of the two (solid curve). The four decay modes (a-d) are the same as in Fig. 4.

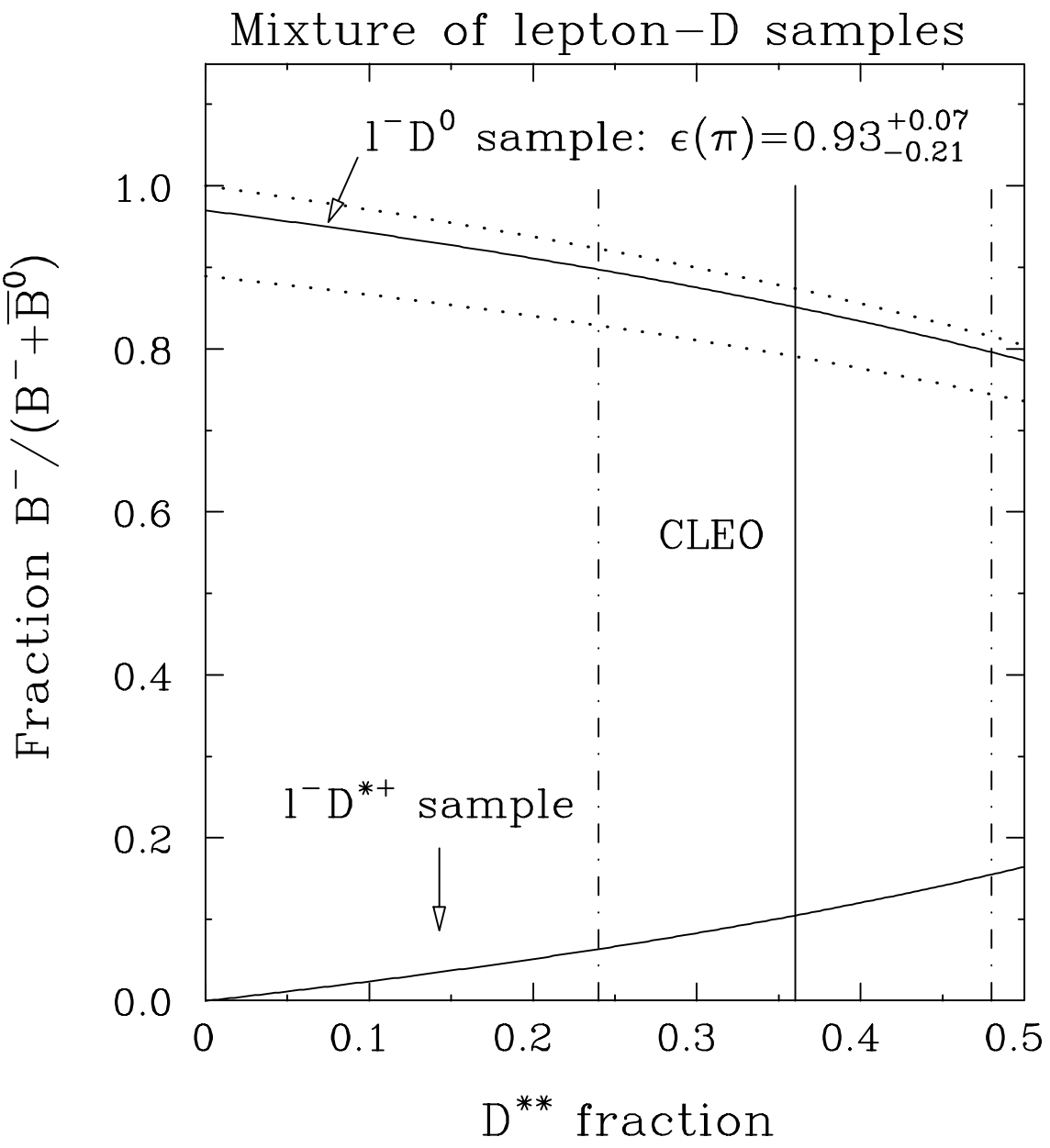

FIG. 7. Fraction g^- of B^- mesons in lepton-$D^{(*)}$ samples as a function of the D^{**} meson fraction f^{**} in semileptonic B decays. Vertical lines show the range of CLEO measurement [20]. The relative abundance of various D^{**} mesons is fixed to $P_V = 0.78$ (see text). Low energy pion reconstruction efficiency is fixed to 0.93 (solid curves), 0.72 and 1.0 (dotted curves).

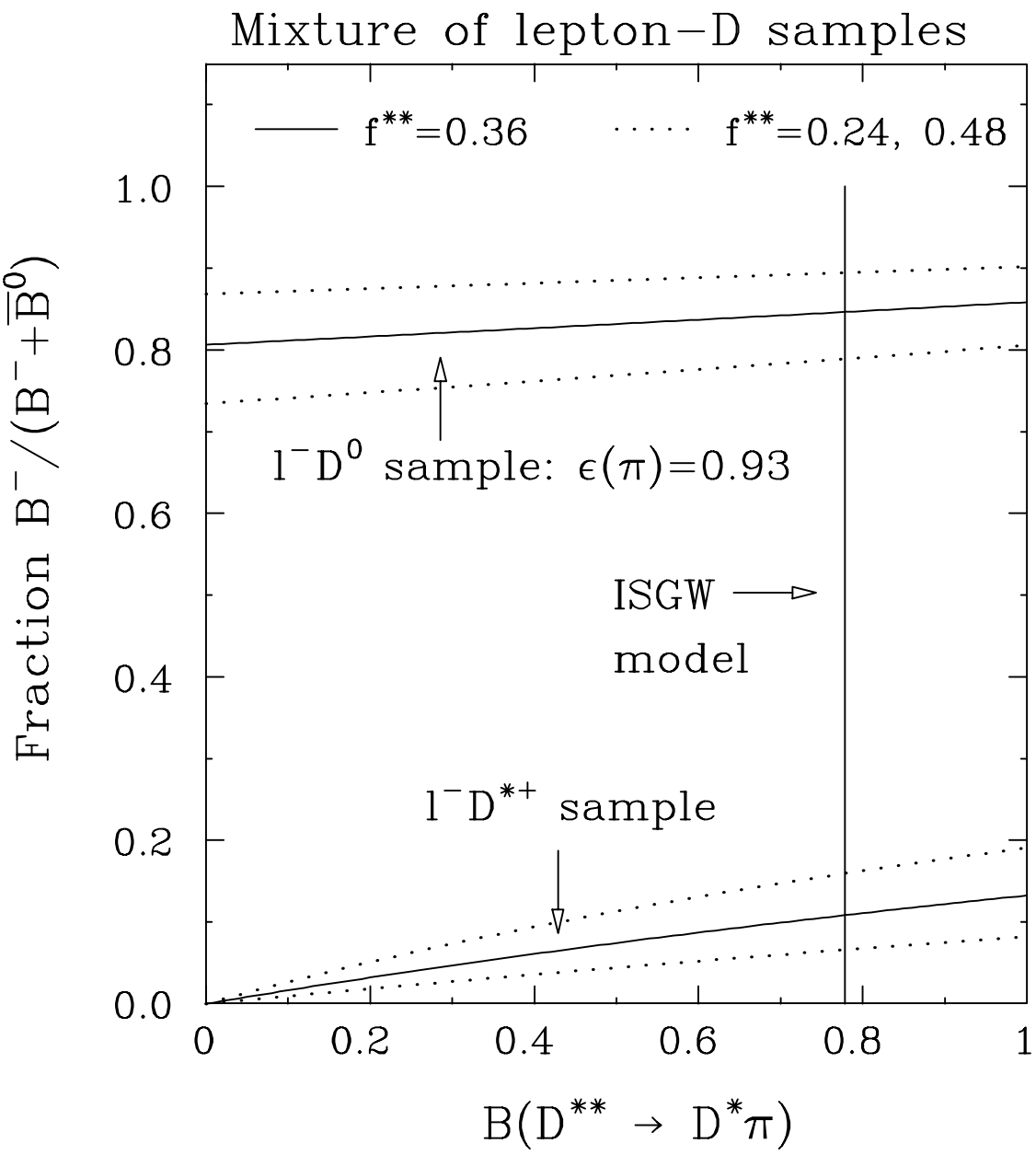

FIG. 8. Fraction g^- of B^- mesons in lepton-$D^{(*)}$ samples as a function of the average D^{**} branching fraction $\mathcal{B}(D^{**} \to D^*\pi)$ or P_V. Vertical line corresponds to the prediction of the ISGW model [18]. The D^{**} fraction (f^{**}) is fixed to 0.36 (solid curves), 0.24 and 0.48 (dotted curves). Low energy pion reconstruction efficiency is fixed to 0.93.

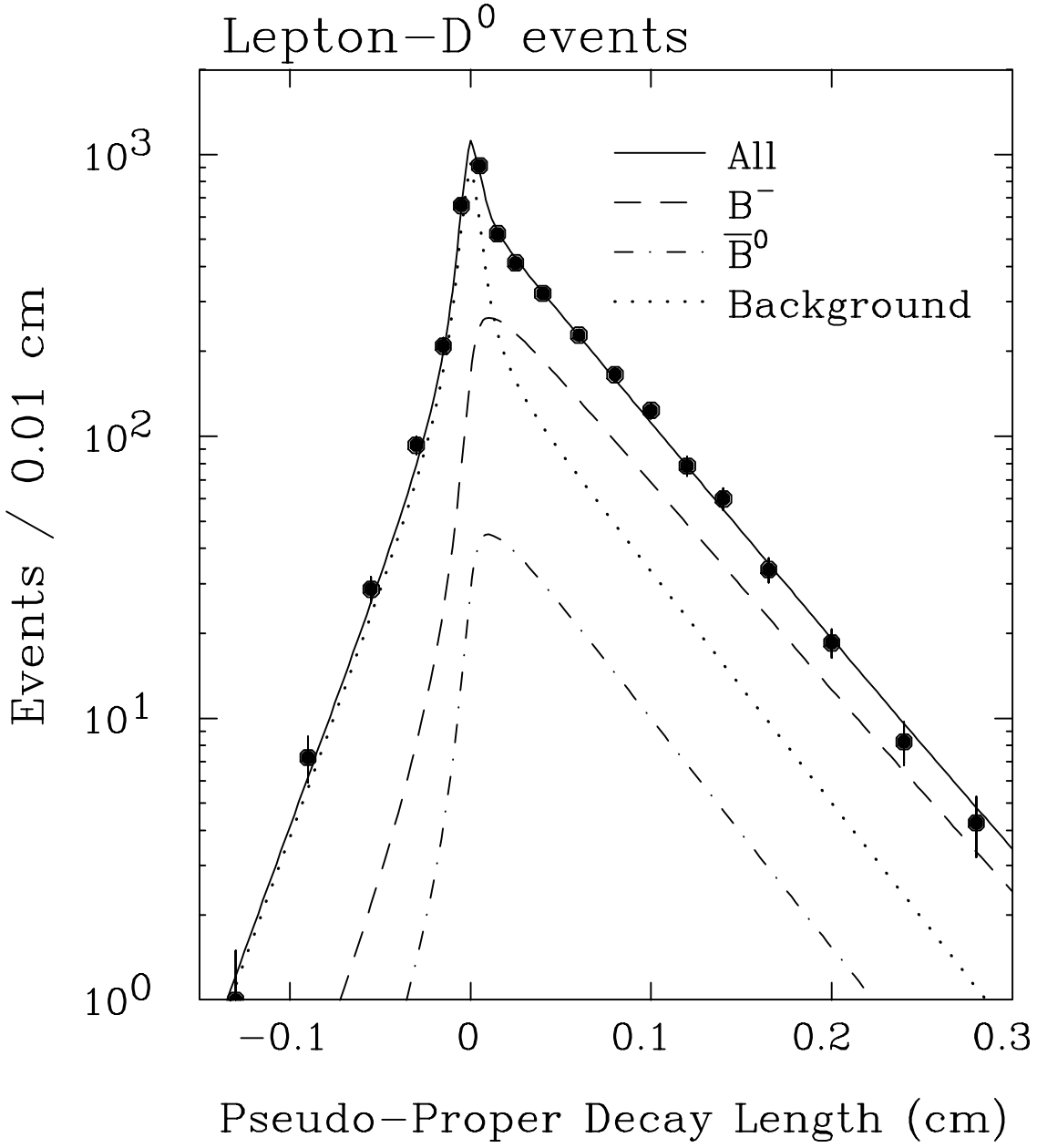

FIG. 9. Pseudo-proper decay length distribution of the $\ell^- D^0$ candidates (points). Curves show the result of the combined fit with $\ell^- D^{*+}$ candidates: The B^- component (dashed curve), the $\overline{B}^0$ component (dot-dashed curve), and the background component (dotted curve).

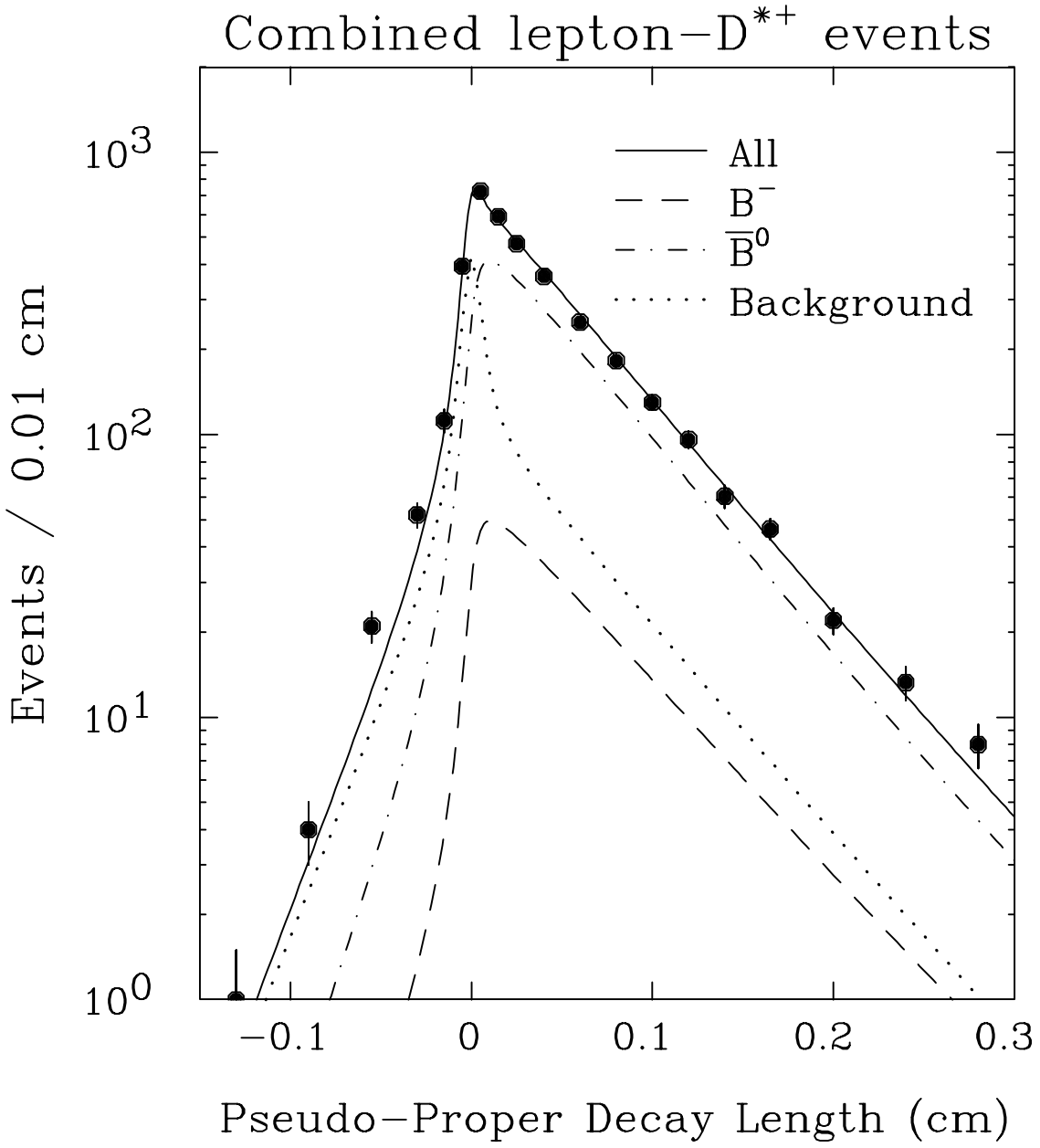

FIG. 10. Pseudo-proper decay length distribution of the $\ell^- D^{*+}$ candidates (points). The three D^0 decay modes are combined. Curves show the result of the combined fit with $\ell^- D^0$ candidates: The $\overline{B}^0$ component (dot-dashed curve), the B^- component (dashed curve), and the background component (dotted curve).